Title
Biomechanical Testing Of An Adhesive Polymer Intended For The Treatment Of Retinal Detachment

Author
Kerr, Mayuri

Publication Date
2014

Peer reviewed|Thesis/dissertation

UNIVERSITY OF CALIFORNIA

Los Angeles

Biomechanical Testing Of An Adhesive Polymer Intended For The Treatment Of Retinal Detachment

A thesis submitted in partial satisfaction

of the requirements for the degree Master of Science

in Biomedical Engineering

by

Mayuri Mohan Panse Kerr

2014

ABSTRACT OF THE THESIS

Biomechanical Testing of an Adhesive Polymer intended for the Treatment of Retinal Detachment

by

Mayuri Mohan Panse Kerr

Master of Science in Biomedical Engineering

University of California, Los Angeles, 2014

Professor Warren Grundfest, Chair

Untreated retinal detachment can lead to blindness. Contemporary treatments involve the use of scleral buckles, or tamponade agents, to appose the retina against the choroid anchor, followed by "welding" the retina to the choroid with laser or cryopexy. While effective at reattachment, these procedures result in the formation of scar tissue that is devoid of function and subjects the surrounding tissue to mechanical strains leading to potential re-detachment. In addition, the scarring of tissue can require several weeks to completely adhere to the underlying ocular tissues, resulting in additional discomfort for the patient. A novel Polyethylene glycol (PEG)-based adhesive polymer, recently developed by Medicus Biosciences, aims to re-attach the retina while avoiding the complications of current treatments. This optically clear, biocompatible adhesive can be applied quickly and will hold the retina in place while retaining function and avoiding the formation of scar tissue. However, to avoid artificial mechanical strains upon the surrounding tissue, the mechanical properties of the polymer must be similar to those of the healthy retina to allow proper healing and

regeneration. The present study is a comparative evaluation of the mechanical properties of the Medicus Polymer to that of healthy intact retinal tissue supported by surrounding tissues. Intact harvested porcine eyes were used for static and dynamic testing of the intact retina, torn retina, and polymer-sealed retina. Our static tests reveal that the Medicus polymer is mechanically stiffer than the intact retina with a Young's modulus of 2160 ± 923 kPa relative to that of the intact retina supported by surrounding tissues at 278 ± 158 kPa. The dynamic testing resulted in a contradictory result with the intact retinal stiffness determined to be 116 ± 72.7 kPa compared to 54.5 ± 25.2 kPa of the polymer sealed retina. The polymer does, however, match the resilience of the retina with the intact retina resulting in 60.79 ± 4.68% compared to the 58.11 ± 12.90% resilience of the polymer-sealed retina. Finally, the yield and failure strengths of the polymer and intact retina were not significantly different.

The thesis of Mayuri Mohan Panse is approved.

Joseph L. Demer

Andrea M. Kasko

Wentai Liu

Warren Grundfest, Committee Chair

University of California, Los Angeles

2014

DEDICATION

To my family and friends. To Professor Warren Grundfest for his support. To Dr. Bryan Nowroozi for his patience, knowledge, insights and encouragement. To Justin Thai for all his hard work and making time in the lab fun. To my wonderful husband Alex Kerr.

TABLE OF CONTENTS

LIST OF FIGURES

LIST OF TABLES

LIST OF ACRONYMS

ILL – Internal limiting lamina

IPM – Interphotoreceptor matrix

PPV – Pars plana vitrectomy

PVD – Posterior vitreous detachment

RPE – Retinal pigment epithelium

SBP – Scleral buckling procedure

ACKNOWLEDGMENTS

Dr. Jean-Pierre Hubschmann for advising on the experimental setup and guiding the experiments, Humphrey Sumner for enabling our access to the microsurgery lab, Logan Hitchcock and Nina Zelcer for ordering and logistics of tissue samples, James Garritano for infecting me with his enthusiasm for MATLAB, Alan Priester for making it possible to use the MakerBot for 3D printing. Dr. Tatsuhiko Sato for doing the isolated retina dissections

Introduction

The retina is an elastic tissue, approximately 250 μm in thickness, that is essential for proper visual function [1]. However, in approximately 12 in every 100,000 cases, the retina detaches from the underlying Retinal Pigment Epithelium (RPE) resulting in patient discomfort and ultimately progressing to blindness [2]. Retinal detachment has a lifetime risk of approximately 5% at 85 years of age with around 20,000 new cases identified every year in the US, and patients having undergone cataract surgery [3], and patients taking certain medications such as oral fluoroquinolones are at a higher risk [4]. While treatments exist for retinal detachment, they are typically prolonged for several weeks to months, and can result in patient discomfort as well as loss of visual function. In addition, current treatments tend to modify the mechanical properties of the intraocular tissues, often times resulting in additional future detachments [3]. An imbalance in the forces that hold the retina in place can lead to retinal tears and detachment, therefore it is important that treatments retain the biomechanical properties of the retina upon recovery. A novel form of treatment has recently been proposed consisting of a hydrogel adhesive that polymerizes *in situ* to reattach the retina. This polymer adhesive attempts to mimic the mechanical properties of the retina to avoid complications associated with current treatment methodologies. The present thesis is a comparative evaluation between the biomechanical properties of this novel polymer and the healthy retina in enucleated, intact porcine eyes. The aim of the thesis is to quantify the biomimetic properties of the polymer relative to the intact intraocular tissues.

Biomechanics in the eye

Various active and passive forces keep the retina attached to the back of the eye. An imbalance in these forces can lead to retinal tears or detachment. These imbalances are often associated with a disruption in the anatomy or physiology in the eye. Therefore a comprehensive understanding of the intraocular anatomy and biomechanical environment are essential to develop novel treatments for retinal tears and detachments.

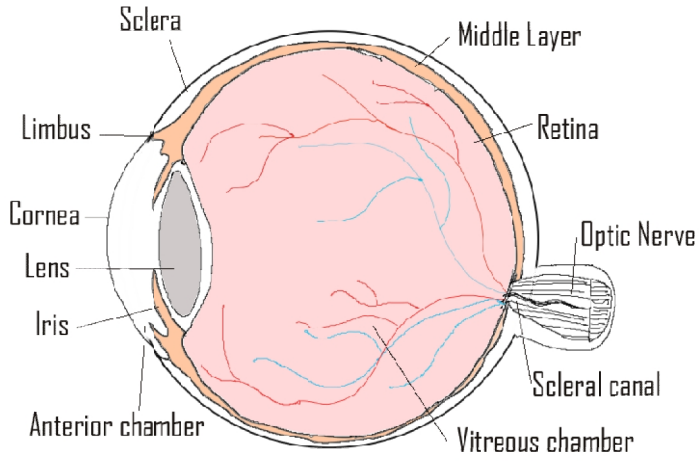

Figure 1. Anatomy of eye (Modified from Brinton D, Wilkinson C. Retinal Detachment: Priniciples and Practice. 2009.)

Anatomy

As seen in figure 1, the retina is a very thin, delicate tissue covering the posterior chamber of the eye. It is apposed in the posterior of the eye to three tissues including the Retinal Pigment Epithelium (RPE), the choroid, and the sclera. The sclera gives the eyeball shape and protection while the choroid has capillaries that nourish the retina. Both the shape of the eyeball, as well as the oxygenation via the choroid, can influence retinal adhesion. The RPE is a monolayer of cells that the retina rests on. It is

10 µm thick and keeps the retina in place through physical interlocking with the outer layer of the retina and active pumping of fluid from the eye [4].

In addition to this peripheral anatomy, the vitreous humor, which fills the posterior chamber of the eye, can also influence retinal adhesion [5]. The vitreous humor is a gel-like network of collagen with interspaces filled with hyaluronic acid polymer [6]. It has high water content (98-99.7%) and is relatively acellular [7]. As seen in Figure 2, the vitreous occupies almost 80% of the eye and can be divided into the basal vitreous, the cortex, the intermediate vitreous, and the central vitreous. Each of these regions is made up of bundles of collagen fibers that adhere to the retina with variable attachment strengths based on their density and fiber orientations. The basal vitreous is an annular zone at the anteriormost extent of the retina, the ora serrata, where dense bundles of collagen fibers adhere to the retina and the fibres are inserted perpendicular to the retina [7].

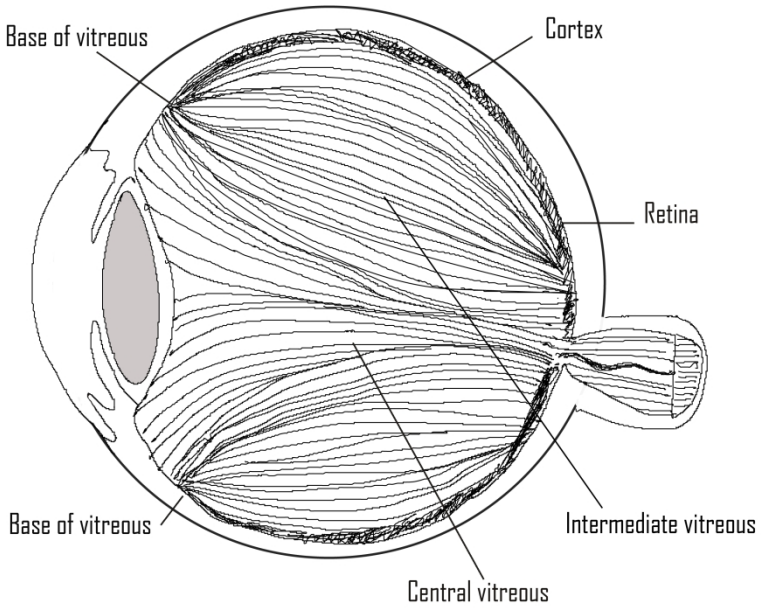

Figure 2. Collagen strand orientation in the vitreous. (Adapted and redrawn from Le Goff MM, Bishop PN. 2008)

Collagen fiber density is lowest in the central vitreous and increases as we go outward. The highest density is found within the vitreous cortex [8]. The cortex of the vitreous is a thin layer (100-300 μm) that surrounds the central vitreous and is characterized by collagen fibrils that mostly run parallel to the retina [7]. The vitreous is attached to the innermost layer of the retina creating the vitreoretinal junction through the cortical vitreous [9]. The cortex is therefore, the strongest part of the vitreous, and the multiple collagen fibers attached to the retina affect retinal detachment and tears. Diseases of the vitreous that cause vitreal collapse put large amounts of traction on the retina [7].

Biomechancis of normal retinal adhesion

The retina is held in place in the eye with several passive and active forces. The passive forces are associated with fluid flow and protein concentrations within the eye that contribute to pressure gradients, and to the relative permeability of the intraocular tissues. The first of these is the oncotic pressure, or osmotic pressure gradients, developed intraocularly due to proteins in plasma [10–12]. Between the sclera and the retina is a layer of blood vessels called the choroid. The capillaries of the choroid have high permeability where protein extravasation occurs causing a higher concentration of proteins relative to that in the plasma. This concentration gradient therefore translates into a pressure gradient across the retina, between the vitreous and choroid. The higher osmotic pressure results in fluid transport outward from the vitreous across the retina and RPE, to be absorbed by the choroid [13–15]. Thus, as a result of the fluid transport across the retina, the retina is apposed against the RPE and choroid.

An additional contributor to this oncotic pressure is the hydrostatic pressure associated with fluid flow from the ciliary bodies [16]. Circulatory components of the

ciliary body push fluid into the posterior chamber of the eye. Fluid in the vitreous chamber then flows outward towards the sclera and is absorbed by the choroid. Intraocular pressure and outflow of water towards the choroid, thus contribute to the hydrostatic pressure gradient that pushes the retina against the RPE and choroid [10], [17, 18]. This transport of fluid radially outwards occurs constantly, and, in rabbits, has been shown to be replaced every 10-15 minutes, corresponding to a total water exchange of about 85 cubic mm [19].

Finally, the retina has a lower permeance to water than the RPE. This is postulated to result from the long and tortuous path water molecules have to take through the ten cellular layers of the retina (approx. 200 µm), compared with the RPE, which is a monolayer of cells approximately 10 µm thick that the retina rests on. This difference in permeance results in the retina impeding the movement of water more than the RPE, effectively pushing it up against the RPE. Thus, the retina and RPE work as one system to create a hydrostatic gradient that drains fluid in the subretinal space, and passively keeps the retina in apposition with the RPE [18]. The pressure difference required to keep the retina in place is very small and estimated to be about 0.52×10^{-3} mm Hg [17].

A second mechanism for keeping the retina in place is associated with the gel-like vitreous humor and its the collagen fiber attachments to the retina. In the normal eye, the vitreous humor acts as a natural tamponade, keeping the retina supported against the back of the eye by occupying the bulk of the space in the posterior chamber in the eye [20].

Along with acting as a tamponade, the vitreous also helps anchor the retina in place via the collagen fiber attachments. The vitreous is postulated to be attached to

the retina at the level of the Internal Limiting Lamina (ILL) which is the innermost layer of the retina [7, 8, 21]. Some authors have suggested fibrillar connections between the ILL and vitreous, while others have suggested that the adhesive between the ILL and vitreous comes from extracellular matrix components [8, 22]. These attachments of the collagen fibres give the retina stability by keeping it in place during eye movement [23]. Since the eye has so many different tissues within it, it is possible that rotational movements would cause structures to move at different speeds and cause friction and tension between the various components. However, during normal eye movements, there is no significant difference in the rotational speed of the central and peripheral portions of the vitreous. This is due to the stabilizing effect of the uniform collagen network in the vitreous gel. Also the inherent viscoelastic properties of the vitreous protect the retina against traction during eye movements [24].

The vitreous also has strong attachments to the retina in the periphery through the retinal capillaries. The vitreous is attached with 'vitreoretinovascular bands', which are strong bands, sometimes as thick as the capillary they are on, which attach the vitreous, the capillary and neighboring retina [25]. These attachments serve to stabilize the retina and the blood vessels within it.

The cortical vitreous also helps mediate retinal adhesion by creating a highly oxygenated zone close to the retina [5]. High local oxygen concentrations help the retina remain adherent and oxygen levels can reversibly affect adhesion [26, 27].

The retina is supported by the RPE and it is an important component of retinal adhesion. The photoreceptors of the retina are the outermost layer of the retina resting on the RPE. The cells of the RPE have villi that wrap around these photoreceptors providing frictional resistance that contributes to keeping the retina adhered to the RPE (Figure 3) [28]. In addition to these villi, the Interphotoreceptor

matrix (IPM), an extracellular matrix which lies between the retina and the RPE, also surrounds the photoreceptor cells [29]. The IPM contains several glycoconjugates that mediate adhesion, and act as a viscous glue keeping the retina attached to the RPE [30]. When the retina is peeled from the RPE, the elastic response of the IPM demonstrates that it is firmly attached to both retinal and RPE surfaces [31]. The IPM macromolecules have been shown to be sensitive to factors such as temperature, pH, and ion concentrations, and therefore, it has been suggested that the sensitivity of retinal adhesion to these factors can be attributed to the IPM [27].

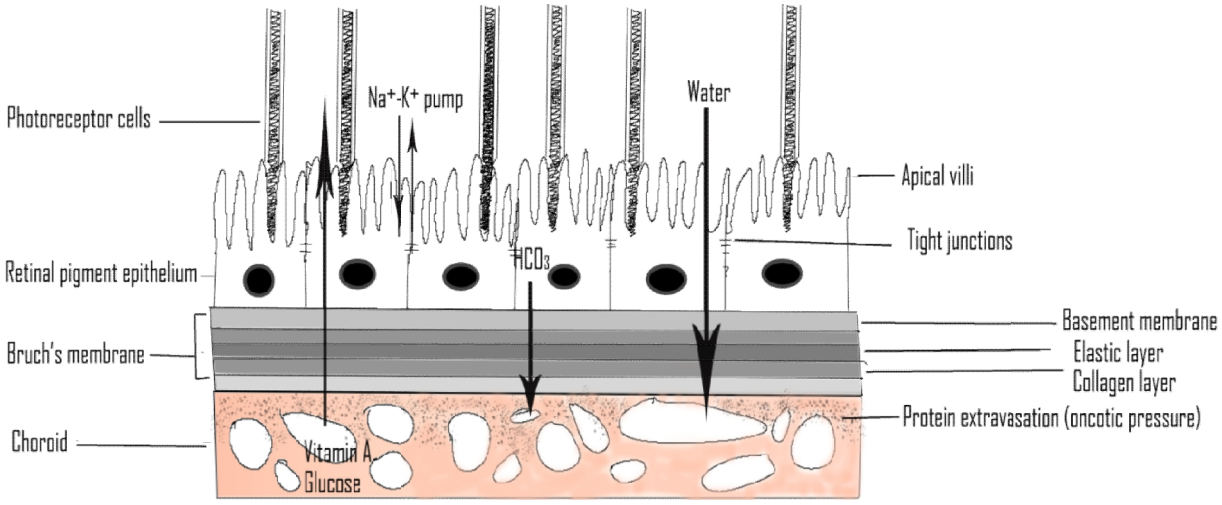

Figure 3. The Retinal Pigment Epithelium (Modified from Steinberg *et al* 1985.)

Finally, active processes are also involved in keeping the retina in apposition with the RPE. Various channels and ion transport mechanisms are present on the apical and basal membranes of the RPE. A sodium-potassium channel is present apically while a bicarbonate channel is present on the basal aspect of the RPE (Figure 3). These channels actively pump ions contributing to osmotic differences across the retina. Net movement of ions and fluid over the RPE contribute to an overall force outward to the choroid and help keep the retina in place [32]. Active ionic transport

comprises 70% of subretinal fluid flow across the RPE resulting in retinal apposition to the RPE and choroid. The remaining 30% is due to the previously described oncotic pressure gradients [33].

Retinal adhesion is also dependent on metabolism and this is seen by the fact that the retinal adhesive force drops immediately post-mortem but can be reversibly modified by an increase in oxygenation [34]. Metabolic inhibitors have also been shown to reduce adhesiveness of the retina [35].

Biomechanics of retinal detachments and retinal breaks

Retinal detachment is a serious condition that is caused by separation of the retina from the underlying RPE. Surgical treatment for retinal detachment depends on type, severity, and location of the detachment. Causes of retinal detachment include inflammatory diseases of the eye, genetics, trauma, myopia and surgery [36]. Each of these pathologies ultimately disrupts the biomechanical forces of adhesion described in the previous section, thereby resulting in retinal detachments [36].

There are three kinds of retinal detachments: Rhegmatogenous, Tractional and Exudative. Rhegmatogenous detachments are the most common (about 90% of all cases) and are caused by a break in the retina that allows fluid to accumulate in the subretinal space, separating the retina from the RPE [36].

Symptomatic posterior vitreous detachment (PVD) often leads to rhegmatogenous retinal detachment. PVD is a process in which the cortical vitreous gel splits away from the Internal Limiting Lamina (ILL) of the retina. Over the course of a person's lifetime, the vitreous gel forms areas of liquefaction as seen in panel 1 of Figure 4 [7].

These small pools of liquefied vitreous form where the normal collagen network structure has broken down (Figure 4, Panel 2) [7]. At the same time, due to the thickening of the ILL, there is a reduction in the ECM components that hold the vitreous adhered to the retina at the posterior pole of the eye and as a result the ILL and vitreous cortex begin to split apart (Figure 4, Panel 3).

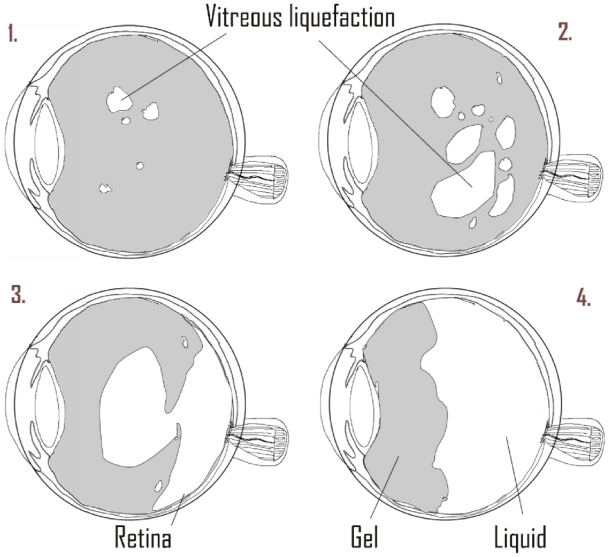

Figure 4. Stages of posterior vitreous detachment (Adapted and redrawn from Le Goff MM *et al,* 2008)

The small liquefied areas coalesce to form a larger pool of fluid which eventually ruptures the vitreous gel, and collapses the structure antero-inferiorly, where the basal vitreous remains attached with its strong collagen fiber adherence to the retina (Figure 4, Panel 4). If the vitreous humor detaches completely from the posterior of the eye, it is termed Complete PVD. However, if any retinal adhesions remain posteriorly, it is considered partial PVD [7, 21, 37].

If attachments of the vitreous to the retina remain, they cause traction as seen in Figure 5 [38]. If an operculum is torn off creating a retinal hole, it generally remains stable since there are no additional forces acting on the hole. However, if a band of

vitreous remains attached to the edge of a flap, it continues to pull away the retina from the back of the eye, enlarging the tear [36].

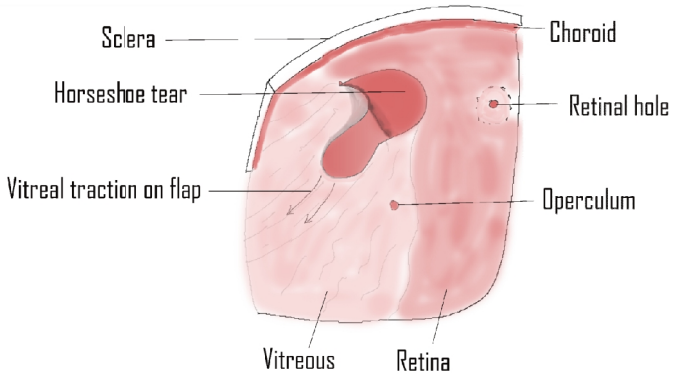

Figure 5. Horseshoe tear with vitreal traction, retinal hole and operculum (Adapted and redrawn from Brinton D, Wilkinson C. Retinal Detachment: Priniciples and Practice. 2009.)

The liquid vitreous further dissects the gelatinous vitreous away from the retina as these structures rotate against one another [39]. The traction generated applies a large amount of force on a small area and retinal tears and detachment follow. The 'vitreoretinovascular bands' that connect the vitreous strongly to the retinal vasculature can cause proliferative or hemorrhagic incidents during PVD or vitreal traction [25, 40].

It has been postulated that if liquefied vitreous after PVD enters the subretinal space through a retinal tear, its albumin content could cause subretinal fluid to persist and cause a retinal detachment [41–43]. However, it is known that not all retinal breaks lead to retinal detachment [37, 44, 45].

Symptomatic PVD can also lead to another form of retinal detachment called tractional retinal detachment. Tractional detachment occurs when pathologic vitreoretinal adhesions pull the retina away from the RPE without a tear in the retina. If

a retinal break develops, it becomes a combined tractional and rhegmatogenous detachment [36]. Retinal breaks can be categorized as primary breaks which are responsible for retinal detachment and secondary breaks that develop in the retina after detachment [36].

In complete PVD, where the vitreous gel has no attachments posteriorly, there is still a possibility of creating traction on the retina. In the intact, healthy vitreous, eye movements do not cause traction on the retina, however, when the collagen network of the vitreous collapses antero-inferiorly during PVD, the remaining space is filled with liquid vitreous. This results in the gel, liquid, and the retina now moving at different speeds during rotation creating traction between the three structures leading to tractional detachment [24].

Lastly, exudative, or serous, detachments are characterized by subretinal fluid accumulation in the subretinal space leading to detachment without a tear in the retina [36]. Water is constantly being pumped through the RPE into the choroid. Any abnormality that affects the outward pumping of water from the eye or the absorption capability of the choroid, leads to an accumulation of fluid in the subretinal space and pushes the retina away from the RPE [46, 47]. This condition is usually caused by an abnormality in the choroid that affects its permeability (*eg.* tumor) or any condition that causes damage to the RPE [36]. For example, trauma can cause a break in the RPE while local hypertensive events that cause a vasoconstriction of the capillaries in the choroid can affect the permeability of the blood vessels [47].

Alternatively, if the RPE is damaged, water is absorbed from the subretinal space into the choroid more quickly [48]. However, the presence of protein in subretinal fluid

slows down the process, and the fluid persists since the RPE does not transport protein into the choroid [41].

Most untreated retinal detachments continue to progress and cause total or near total detachment leading to blindness [36]. Treatments for retinal tears and detachment need to focus on the imbalance of forces that caused it and restore the biomechanical parameters to their physiological levels to be successful and prevent further problems.

Current Treatments

The goal of any retinal detachment treatment is to find all possible retinal separations and tears, remove the cause of detachment or tearing, reposition the retina against the back of the eye, seal those retinal lesions and remove any causes for further tears or detachment.

Current treatments for Retinal detachment (RD), depending on the cause, range from scleral buckling, intraocular gas or silicone oil tamponade with or without vitrectomy, cryotherapy, laser photocoagulation, and if required, drainage of subretinal fluid [49, 50].

Most cases are first treated with a vitrectomy to prevent traction on the retina and further detachment. Once the vitreous is removed, the retina is pushed back into place by using heavy perfluorooctane fluids, gases (sulfur hexafluoride or perfluoropropane), or silicone oil. The gas or fluid is injected into the vitreous space. Gases generally are resorbed over a period of days [51]. The silicone oil is retained in the eye and has to be removed once the retina is believed to have reattached [36].

An alternative method of retinal apposition to the RPE is the use of a Scleral buckle. The buckle functions as an episcleral explant, providing external indentation to change the shape of the eyeball, and to appose the retina. The scleral buckle is often positioned above the tear to push that part of the eyeball inwards, relieving any tension that vitreal bands are exerting on retinal tears. This helps counteract the internal vitreoretinal traction. It also helps appose the RPE with the detached retina after a vitrectomy has been performed by bringing the two tissues closer physically [36].

Once the retina is positioned against the back of the eye, laser retinopexy, or cryopexy, are performed to hold the detached retina in place, or to seal a retinal tear. Laser retinopexy uses extreme heat, while cryopexy uses extreme cold, to create controlled burns on the retina leading to the eventual formation of chorioretinal scars [36]. A series of small burns are made in a radial orientation surrounding the tear to adhere the layers together with subsequent formation of scar tissue [6]. After a laser burn, the RPE is able to heal itself and resume transport of subretinal fluids, thus keeping fluid from accumulating [32]. In fact for about two weeks after a laser burn, due to damage to the RPE, non-proteinaceous fluids in the subretinal space are cleared faster [52, 53, 54].

Complications resulting from current treatment

The procedures currently used to treat retinal detachments and tears have several drawbacks. Vitrectomies have been associated with a variety of complications including the development of cataracts [49]. One possible reason is that the vitreous controls oxygen concentration in the eye and its absence leads to a higher oxygen environment around the lens leading to cataract formation [55]. Vitrectomy itself puts traction on the retina and could cause further detachment or tearing [56].

Suprachoroidal hemorrhage is also a complication during or after vitrectomy with increased risk for patients with old age, high myopia, aphakia or pseudophakia, retinal detachment, and scleral buckle [57]. During vitrectomy, often the inner limiting lamina is removed. The ILL contributes to the structural stability of the retina and it has been observed that the central part of the retina, the macula, becomes more mobile and easily engaged with the vitrectomy aspirator [23].

Scleral buckling comes with a different set of complications including buckle intrusion, buckle protrusion, breakage and buckle-related infection often times leading to redetachment [58, 59]. One of the most common problems associated with scleral buckling is modulation of the geometry of the eye causing postoperative refractive errors. In addition, there can be extraocular muscle imbalance leading to strabismus, commonly known as squint eye [58]. Finally, serous choroidal detachment, which is caused due to accumulation of fluid between the choroid and sclera, displacing the choroid, is a very common problem and seen in 23% to 44% of eyes undergoing scleral buckling [60]. Silicone in the form of silicone sponge or silicone rubber is often used as buckle material, however, the incidence of infections requiring removal is high [61].

Complications associated with the use of gas tamponade agents involve patient discomfort as well as possible subretinal fluid accumulation and possible redetachment [62]. The use of gas tamponade agents in the vitreous space to hold the retina in place requires the patient to be in a face-down, or prone, position for several days until the gas is resorbed to ensure proper healing. If the bubble moves away from the break or detachment, subretinal fluid can accumulate worsening the condition. There is also the possibility of gas leaking into the subretinal space [62].

Similar to gas, patients treated with silicone oil tamponade agents must maintain a prone position as well. In addition, silicone oil causes complications, such as glaucoma, cataracts, corneal degeneration, and emulsification [63]. Morevoer, silicone oil must be removed once healing is complete, as it is not absorbed. Therefore, a follow up procedure is necessary [36]. In one study, 100% of patients over a 10 year period suffered from cataracts in the eye after removal of silicone oil [64]. Although silicone oil is a relatively safe vitreous substitute, it may flow into the anterior

chamber, subretinally, or even out of the eyeball, and result in difficult removal because of the free fluid characteristics within the eye in silicone oil–filled eyes resulting in inflammatory responses [63].

Laser retinopexy and cryopexy cause burns that involve the choroid, the RPE and the photoreceptor cells [65]. This means that those photoreceptor cells are damaged and no longer functional. Also the scar tissue that forms after healing is collagen-dense and has been shown to be stiffer than that of the surrounding retina [54]. In one study, the scars were found to have an adhesiveness which was 220% more than normal retinal tissue after laser and cryopexy [54]. While additional adhesiveness may seem beneficial, if the surrounding tissue is not similar, the scarred areas create further strains on normal tissues that may lead to re-detachment.

While most treatments strive to achieve a balance in the biomechanical forces, most current treatments are not able to fulfill that need, often times leading to redetachment. Re-detachment due to failed procedures adds to the time and money spent on treatment along with a potential loss of vision. Thus, future treatments should aim not only to adhere the torn retina to the RPE, but also to retain or mimic the biomechanical properties of the intact retina.

Reattachment with Polymer

Bioadhesives to keep the retina in place and to seal tears is an attractive idea. Bioadhesives interact with tissue and stay in place in one of the following ways: mechanical interlocking, intermolecular bonding, chain entanglement, or electrostatic bonding [67]. Mechanical interlocking occurs by the adhesive penetrating into the irregularities and pores of the tissue and locking into the roughness of the substrate. Intermolecular bonding happens by interaction of the molecules/atoms of the adhesive and the tissue. This includes forces like covalent, ionic, hydrogen bonds, dipole interactions and van der Waals forces. Chain entanglement of the bioadhesive polymer chains and the glycoprotein polymers of the tissue creates a 1 – 100 nm contact layer of interpenetrated polymer chains. Electrostatic bonding occurs due to a charge built up by transfer of electrons between the adhesive and substrate [66].

Several tissue adhesives have been tried in the eye. Cyanoacrylate was tried to seal retinal tears however, it stiffens the retinal tissue and causes necrosis under the glue and in adjacent areas. Some of these effects might be due to the exothermic reaction of setting of cyanoacrylate and the toxicity of its breakdown products [67]. Bioadhesives based on fibrinogen, platelets and thrombin have also been tried [66]. However, they have the potential to elicit inflammatory and allergic reactions In addition, these bioadhesives create a chorioretinal scar which has no function, and also has a different biomechanical behavior than the surrounding tissue [66, 68].

Various kinds of hydrogels have also been used. The properties of hydrogels can be modified substantially by changing their composition to suit their intended purpose. However, the monomers and degradation mechanisms of the previously used

hydrogel adhesives impaired healing, and caused inflammatory and allergic responses [69, 70].

Considering all of these issues, a biocompatible hydrogel polymer was developed by Medicus Biosciences to glue the retina back in place without damaging the cells and permitting healing [71].

Polymer chemistry and working details

The Medicus polymer was created from solutions of Polyethylene glycol (PEG) 8-arm acetate amine combined with solutions of PEGylated 8-arm ester dissolved in physiological buffer solution with a viscosity enhancer. It is possible to tune this polymer to vary gelation time from 20 sec to 10 mins. The formulation used for these experiments had a mixing time of 20-30 seconds and a gelation time of approximately two minutes. Its pH is in the range of 6-8. The mechanical properties of the polymer can also be tuned by modification of the number of arms, molecular weights between the arms, and solution concentrations. It is optically clear and can be delivered either via intravitreal or subretinal injection [71].

PEG is an FDA approved polymer of ethylene glycol $HO - (CH_2 - CH_2 - O)_n - H$ where n is the average number of ethylene glycol units present. PEG polymers are commonly used in biological applications as they can form biologically compatible polymers. A surface modified with PEG resists cell and protein adsorption and becomes non-fouling. PEG hydrogels help in wound healing and reduction of scarring, in addition, the reaction of their formation is mild enough to carry out the hydrogel formation *in situ* [72]. The bioresorbable form of this polymer would be useful for treating a detached or torn retina, particularly if the polymer can be formulated to mimic the biomechanics of the retina [71]. PEG is cleared through renal excretion and has a very good safety profile [73].

Thus, the aim of this thesis is to evaluate the polymer and compare the biomechanical parameters of the intact retina with the biomechanics of the polymer-sealed retina. If the polymer is used in place of laser or cryopexy it offers the possibility of the retina being able to heal with minimal scarring. It also prevents the larger issue of causing a mismatch in the biomechanical parameters in the surrounding tissues that could lead to further detachment.

Due to the polymer being a proprietary product, it is not possible to elucidate the exact components. Broadly, the hydrogel is formed by the reaction of a PEG 8 arm ester with a PEG 8-arm amine [74].

Advantages over conventional methods

Hydrogels are very close to the vitreous in nature and being optically clear would be an ideal substitute if used in place of silicone oil. If made bioresorbable, they will be able to allow tissue to heal and there will be no necessity to have a second procedure to remove them, and any associated complications will be prevented [63], [64]. The polymer can be tuned to remain within the eye for as little as 5 days to as long as several months [71]. Degradation occurs primarily through ester bond hydrolysis and there may be enzymes in the eye that would contribute to the degradation. This can be controlled by increasing the number of ester groups for faster degradation, or increased crosslinking, to increase longevity as a gel and slow down degradation [72, 73]. The polymer can also be used as a drug-delivery device in the difficult to reach posterior part of the eye to ensure local delivery of drugs without systemic administration. Since it is a biocompatible adhesive, it will not destroy photoreceptors in the area. Also in cases where the vitreous is mostly healthy and the problem is only a tear in the retina, subretinal application of the adhesive may help avoid additional surgical procedures like vitrectomies.

The Medicus Biosciences polymer is a two part system which can be mixed prior to application and applied to the torn retina where the polymer cures in situ and adapts to the local anatomy.

Biomechanical testing of polymer

Several previous studies have looked at the biomechanical properties of the retina, however, all of them involved cutting open the eye, decanting the vitreous, and measuring the properties of strips of retina excised from the eye. Therefore, to date, no studies have been performed with the retina intact within a whole-eye preparation. In addition, these previous studies were done using varying dissection techniques and tested the retina under different conditions [75-79].

Previous studies conducted static testing of the isolated retina by applying a uniaxial force and investigated the environmental effects of temperature, salinity, and hydration on the mechanical properties of the retina revealing that the post-mortem retina reversibly loses its stiffness at higher temperatures. In saline at 37º C, the modulus of porcine retina was reported to be 11.12 ± 6.10 kPa compared to 111.25 ± 88.16 kPa in room temperature (25º C) saline [75, 76]. The effect of the presence of blood vessels and their orientation in the sample on the elastic modulus was also studied. It was seen that the presence of blood vessels in general makes the retina stiffer and also that larger blood vessels affected the modulus more than smaller ones [77].

It was also seen that depending on the orientation of dissection of the retinal strip, and hence the direction of force applied, significantly changed the modulus. A retinal strip excised in the superior-inferior (vertical) direction had a modulus of 107.8 ± 58.0 kPa compared to a strip excised in the naso-temporal (horizontal) direction

which had a modulus of 73.2 ± 69.8 kPa [76]. Another study used excised retinal strips that were stretched to failure and reported an elastic modulus of 100 – 110 kPa [78]. A recent study measured the elastic modulus of the isolated retina in compression and reported values of 10.5 ± 2.67 kPa [79]. However, none of these values were reported from whole eye preparations. All of these studies were done on porcine retina excised from the eye in strips and reported values ranging from 10 kPa to 110 kPa [23, 75–79]. Through these studies it was clear that in excised pieces of retina, the temperature, kind of dissection, method of testing, presence/absence and orientation of blood vessels, direction of testing and which area the tissue was obtained from gave a range of results [1, 23, 75, 76, 80].

None of the previous studies took into account the support of the surrounding tissues and the fact that the retina does not exist in isolation. Even post-mortem, the eye remains a pressurized globe and opening up the eyeball brings that pressure down to atmospheric pressure. It has been seen in past experiments that even a small opening made for introduction of a micropipette leads to spontaneous detachments possibly due to the sudden drop in intraocular pressure [48]. To this end, we used intact porcine eyes to ensure that the intraocular pressure did not change and the retina was tested as it normally exists, surrounded by other tissues.

Our experiments were set up to test the retina *in situ* with all the surrounding tissues intact. This is especially important from the clinical point of view since the retina is never isolated and is in constant contact with other tissues and affected by forces originating from them in the intact eye. Removing the retina from the structure of the eye changes its environment drastically to a degree that might leave the data biologically irrelevant.

The biomechanical parameters that were looked at were elastic modulus, yield and failure strength through static testing and hysteresis/resilience by dynamically testing the intact retina and comparing it to the polymer sealed retina.

Stress can be defined as the force exerted per unit of cross-sectional area. In this case, the cross sectional area was the tip of the tapered tip plunger and stress was measured by the muscle motor. The strain was calculated by the change in displacement of the plunger.

$$Stress = \frac{Force}{Area} \qquad Strain = \frac{Change\ in\ length}{Original\ length}$$

The elastic modulus was calculated by the formula and was selected by clicking a point on the stress-strain graph and the slope calculated in MATLAB.

$$Elastic\ modulus\ = \frac{Stress}{Strain}$$

The Yield strength is the point beyond elastic (reversible) deformation at which a material begins to plastically deform. After this point, removal of the forces acting on it will not completely reverse the deformation in the material.

The Failure strength is the force at which the material tears or breaks. Hysteresis is the loss of energy during deformation and subsequent return to original form. It depends on the rate of loading and unloading and is the energy absorbed by reversed deformation. Hysteresis was calculated by taking the integral of the load curve for a given cycle and subtracting the integral of the unload curve for the same cycle.

Resilience can be thought of as the energy returned to the system for each cycle of loading. Resilience was calculated as 1-Hysteresis.

While it is true that in eyes being treated for retinal detachments and/or tears, a vitrectomy is usually involved, the elastic modulus of the vitreous has been reported to be between 1-3 Pa [81, 82] so it is unlikely that the presence of the vitreous would greatly affect the measured values for the elastic modulus of the retina which have been reported to be in the 10-110 kPa range [23, 75, 76, 78, 79].

We designed an experiment involving the creation of a small scleral window near the posterior pole of the eye with minimal dissection. The retina was tested for its mechanical properties in a nearly intact eye and placed in a Balanced Salt Solution bath to better mimic physiological conditions. The part of the eye above the level of the solution was constantly kept moist by using a syringe to drip BSS on the eye. Keeping the entire system intact helped us assess the elastic modulus of the retina with an intact vitreous supporting it and then compare it to the polymer without any removal of tissue from eye. This helped fulfill the aim of the thesis which was comparison of the biomechanical parameters of the intact retina supported by surrounding structures and the torn retina sealed with the polymer.

To compare the values recorded from testing the intact eye with the isolated retina, a separate set of experiments was conducted by isolating the retina from the surrounding tissues and testing the tissue immersed in BSS.

Materials and methods

A dual-mode servomotor muscle motor (305C-LR, Aurora Scientific, Aurora, CA) was used to measure the force resulting from controlled displacement of the tissues. The system consisted of the motor, a desktop computer and software from Aurora Scientific accompanying the muscle motor. Two plungers were 3D printed on the MakerBot Replicator 2 using PLA to desired specifications. One plunger with a tapered tip with a cross-sectional area of 0.7 mm^2 was used for static testing while a flat ended plunger with a cross-sectional area of 11.32 mm^2 was used for dynamic testing (Figure 6).

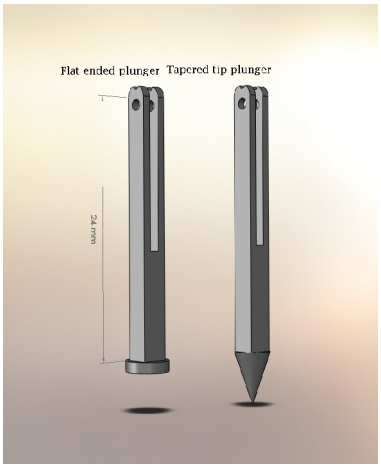

Figure 6. 3D printed Plungers for dynamic (flat ended) and static testing (tapered tip)

The muscle motor itself was screwed to a metal plate that was mounted on a custom built heavy base to secure the motor and prevent any vibration or movement during operation. (Figure 7)

Whole eye experiments

Specimen preparation

The experiments were conducted on fresh pig eyes (n = 100) which were obtained from Sierra Medical (Whittier, CA). The eyes were used within 48 hours of arrival and refrigerated overnight. Specimens were always allowed to warm to room temperature prior to testing, and were never frozen.

Episcleral tissue and ocular muscle tissue were removed with a #10 scalpel and toothed tweezers. A scleral window was created in the back of the eye within a 12 mm radius of where the optic nerve entered the eye. A 5 mm biopsy punch was used to create a deep outline in the sclera and the circular window was carefully dissected using a #11 scalpel to remove the sclera and underlying choroid, revealing the RPE and retina. The RPE was kept intact because it was observed that removal of the RPE resulted in the residual intraocular pressure pushing the vitreous out and tearing the fragile retina.

Eyes that acquired any accidental tears in the retina during creation of the window were discarded. These were easy to find since the vitreous immediately formed a clear bead on the surface of the dark RPE.

Specimen mounting

The eyes were held securely in place with a custom-made holder ensuring that the change in diameter after clamping was minimal (Figure 7). The holder consisted of a heavy metal base and brackets to thread a dental matrix band (Deepak Products Inc, Miami, FL) which was 0.25 x 0.015 inches which could be adjusted to accommodate the varying diameters of the individual eyes. As seen in figure 7, the eye and holder were

placed in a beaker of Balanced Salt Solution and constantly bathed at room temperature to prevent drying of the tissues.

The eye is not a perfect sphere and the major and minor diameters were measured with a Vernier caliper in the position the eye was clamped and the diameters averaged. This was done to ensure that we did not apply excessive pressure from the outside while clamping the eye. The plunger was positioned so it was just touching the retina and the lever arm of the motor was at 90˚ to the plunger.

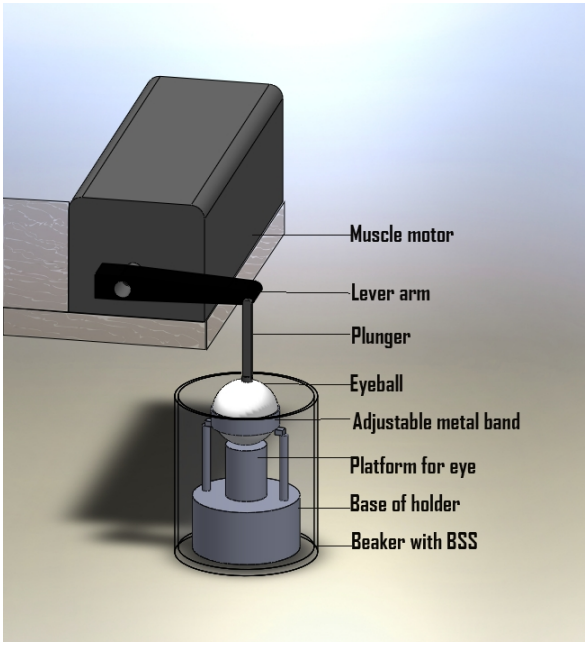

Figure 7. Schematic of the Experimental Setup for whole eyes

Static testing of whole porcine eyes

Static testing of the intact retina and the polymer sealed torn retina were done by pushing the tissue to failure through a set displacement and measuring the force that was required. Static testing was done to determine the elastic modulus, yield

strength and failure strength of the intact retinal tissues and the polymer sealed retina. All the tests were carried out using the tapered tip plunger positioned perpendicular to the exposed retina in the center of the scleral window.

Experimental design

The plunger was pushed to 10 mm since it was observed that the retina failed between 7-9 mm displacement of the lever arm.

Intact retina (n = 18)

To test the intact retina, the plunger was depressed by moving the muscle motor lever arm 10 mm over 5 seconds causing tissue failure evidenced by a tear in the retina. The changes in the displacement and force applied were recorded at a sampling frequency of 1000 Hz.

Polymer-sealed retina (n = 21)

To test the polymer sealed retina, a #11 scalpel was used to make a 1 mm tear in the retina at the center of the window, and the Medicus Biosciences Polymer was applied to the tear. The formulation used for consisted of two syringes, the first filled with an opaque white powder and the second syringe filled with liquid. The two syringes were screwed together, the liquid was pushed into the syringe containing the powder, and the plungers used to agitate the mixture by alternately pushing it into each syringe. Upon mixing for 25 seconds, the polymer was applied onto the exposed retinal tear. Once curing began, 5 mins were allowed for the polymer to set after which the plunger was positioned just touching the surface of the polymer and the test run again.

The polymer sealed retina was displaced to failure and the forces required to do so were recorded. The elastic moduli, yield strength and failure strength of the intact retina and polymer were calculated.

Calculations

Data from each sample consisted of force, position/displacement and time. The data was processed using MATLAB (MathWorks, Natick, MA). A Butterworth filter was used to remove noise in the dataset with a cutoff frequency of 25 Hz. Filtered data was plotted using MATLAB code to produce a stress-strain graph. Stress was calculated by dividing the force measured by the area of the plunger tip, while strain was calculated by a change in the displacement measured by the muscle motor.

Tissue strain was calculated based on motor arm displacement calibration using digitization of visual markers on either side of the plunger. Four markers were made on the retina exposed in a scleral window and the isolated retina, and distances between each pair of points were measured using ImageJ (NIH). The measurements were made for each 1 mm of the 10 mm displacement of the muscle motor arm. These points were considered ends of two axes of an ellipse and the area change between displacements was calculated. The change in area was plotted against the displacement, using a quadratic equation, which was then used as a calibration to calculate tissue strain for the static testing experiments.

Stress can be defined as the force exerted per unit of cross-sectional area. In this case, the cross sectional area was the tip of the tapered tip plunger and stress was measured by the muscle motor. The strain was calculated by the change in displacement of the plunger.

The elastic modulus was calculated by plotting the stress-strain graphs using MATLAB and selecting a point on a graph from which slope was calculated.

The stress–strain curve is thought to have three phases [83, 84] (Figure 8):

- Toe region: This region shows an initial low-strain phase .
- Heel region: There is a gradual increase in the slope of the stress–strain curve caused by increasing stress and it is seen as a concave, non-linear area of the graph.
- Elastic region: This is the final phase that leads to the yield point. With increasing strain, the slope remains constant and a linear stress–strain curve is seen.

The point was selected in the linear, elastic region of the graph after the concave 'heel' region of the graph had ended. This was done since the linear region of the graph represents the elastic region of the tissue and points picked anywhere along this line will give the same relationship of stress/strain [84]. The MATLAB code divided the stress by strain at the selected point to give the elastic modulus. The yield and failure points were also selected on the graph (Figure 8).

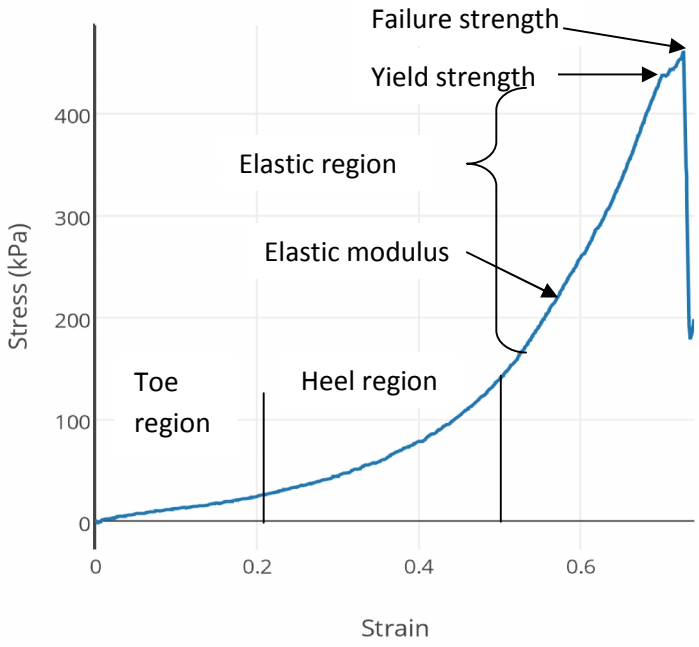

Figure 8. Example graph showing where points were picked for elastic modulus, yield strength and failure strength for each specimen

The Yield strength is the point beyond elastic (reversible) deformation at which a material begins to plastically deform. After this point, removal of the forces acting on it will not completely reverse the deformation in the material.

The Failure strength is the force at which the material tears or breaks.

Statistical analysis

A Student's T-test was conducted to compare the intact retina with the polymer sealed retina.

Dynamic testing of whole porcine eyes

The whole eye specimens for dynamic testing were prepared and mounted as described above for the static tests.

Diameters of whole eyes with prepared scleral windows were measured and the eyes clamped in place in a bath of balanced salt solution. The diameter was measured again to ensure too much pressure was not applied and the intraocular pressure was not raised. Once clamped, the eye was used for testing of the intact, torn and polymer sealed retina.

Experimental design

Dynamic testing involves loading the tissue close to its failure point. Since we had observed the retina and polymer failing between 7 – 9 mm, dynamic testing was performed with cyclical loading for 20 cycles to 6.5 mm displacement at a frequency of 2 Hz and the data was recorded at a sampling frequency of 1000 Hz.

Only the whole eyes with scleral windows were tested this way. When the isolated retina was subjected to cyclic loading, it tore within the first two cycles.

Intact retina (n = 19)

The flat plunger was positioned so it was just touching the retina exposed in the scleral window and the arm of the motor was at 90 degrees to the plunger. The test was run for a 6.5 mm displacement 20 cycles and the results recorded.

Torn retina (n = 19)

A 3mm tear was made in the retina of the clamped eye with a #11 scalpel. The flat plunger was positioned so it was just touching the retina and the arm of the motor

was at 90 degrees to the plunger. The test was run for 20 cycles and the results recorded.

Polymer sealed Retina (n = 19)

After the torn retina was tested, the Medicus polymer was applied to the tear. The formulation used for these experiments came in a vacuum packed packaging of two syringes with a syringe filled with an opaque white powder and the second syringe filled with liquid. The two syringes were opened and their open ends screwed together. The liquid was pushed into the syringe containing the powder and the plungers used to agitate the mixture by alternately pushing them into each syringe. After mixing them thus for 25 seconds, the polymer was applied drop-by-drop on the exposed retina. Once gelation began, 5 mins were allowed for the polymer to set after which the flat plunger was positioned just touching the surface of the polymer and the test run again.

Calculations

Tissue and polymer strain was calculated based on digitization of visual markers on either side of the plunger. Four markers were made, and distances between each pair of points were measured in ImageJ software, a Java-based image processing program developed at the National Institutes of Health. The measurements were made for each mm of the 6.5 mm displacement of the muscle motor arm. These points were considered ends of two axes of an ellipse and the area change between displacements was measured. The change in area was plotted against the displacement. A quadratic equation was used to fit a curve and this was used as calibration for the strain.

The data was exported to MATLAB and the 15th cycle of each test was selected for analysis. Force measured during this cycle was divided by the cross-sectional area of the plunger (11.32 mm^2) to give the stress and the changes in displacement were used to output strain.

Dynamic testing was performed on the normal retina followed by testing the torn retina and polymer sealed retina. This helped quantify the elastic hysteresis and resilience of the tissues and the polymer.

Hysteresis is the loss of energy during deformation and subsequent return to original form. It depends on the rate of loading and unloading and is the energy absorbed by reversed deformation. Hysteresis was calculated by taking the integral of the load curve for a given cycle and subtracting the integral of the unload curve for the same cycle.

Resilience can be thought of as the energy returned to the system for each cycle of loading. Resilience was calculated as 1-Hysteresis.

The elastic modulus was calculated by plotting the stress-strain curves. The area enclosed by the loop, created by loading and unloading of the tissue or polymer, gave the hysteresis and resilience expressed as percentages.

Statistical Analysis

The Young's moduli, hysteresis and resilience collected during testing were evaluated with a Repeated Measures ANOVA for an effect of treatment on each sample. Results give an overall effect at the level of $p<0.0001$. A Tukey HSD posthoc analysis was then done for pairwise comparisons.

Isolated retina experiments

Specimen preparation

After removal of episcleral tissue, the eye was dissected in a circle about 3-4 mm away from the limbus to exclude the ora serrata. Once the cornea and attached sclera were removed, the lens and vitreous were carefully decanted to leave the retina attached in the remaining cup of the eye. A 5 mm biopsy punch was used to make a punch cut around the optic disc. BSS was injected subretinally to separate the retina from the underlying tissues. The eye cup was tipped over and the retina was gently allowed to slide into BSS.

Specimen mounting

A custom perforated hollow cylinder was 3D printed with PLA using the MakerBot Replicator 2. The inner diameter of the cylinder was 10mm and the outer diameter was 14mm. Cyanoacrylate glue was applied to the rim of the cylinder and inverted onto the isolated retina to fix the retina in place. The cylinder was then clamped to the previously described holder to prevent any movement during testing and the whole assembly submerged in BSS (Figure 9)

The data was processed using MATLAB (MathWorks, Natick, MA). A Butterworth filter was used to remove noise in the dataset with a cutoff frequency of 15 Hz for the isolated retina. Filtered data was plotted using MATLAB code to produce a stress-strain graph. Stress was calculated by dividing the force measured by the area of the plunger tip, while strain was calculated by a change in the displacement measured by the muscle motor.

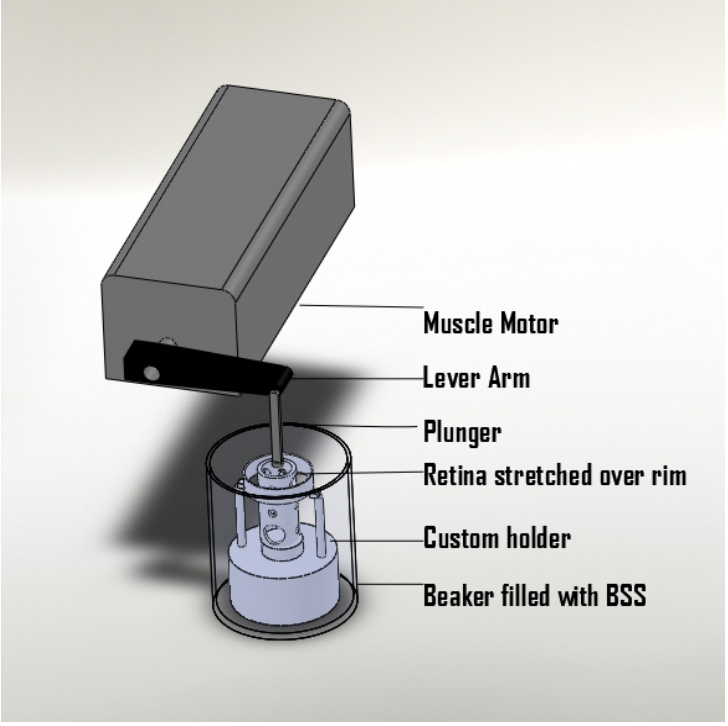

Figure 9. Schematic of the Experimental Setup for testing the isolated retina

Experimental design

The parameters for testing the isolated retina were the same as those for the static testing of whole pig eyes.

Intact retina (n = 18)

The tapered tip plunger was positioned to just touch the isolated retina which was stuck with cyanoacrylate to the rim of a hollow cylinder. The plunger was depressed by moving the muscle motor lever arm 10 mm over 5 seconds causing tissue failure evidenced by a tear in the retina. The changes in the displacement and force applied were recorded at a sampling frequency of 1000 Hz.

Polymer-sealed retina (n = 18)

For the polymer sealed isolated retina, the retina was stuck to the rim of a hollow cylindrical holder and a #11 scalpel was used to create a 1 mm long tear in the center. The two syringe contents were mixed and 0.5 mL of the Medicus Biosciences Polymer was applied to the tear and to evenly cover the entire surface of the retina. After the curing period of 5 mins, the polymer and retina were pushed to a 10mm displacement over 5 seconds. The data collected was then used to measure the elastic modulus, yield and failure strength of the intact retina and polymer sealed retina.

Calculations

Data from each sample consisted of force, position/displacement and time. The data was processed using MATLAB (MathWorks, Natick, MA). A Butterworth filter was used to remove noise in the dataset with a cutoff frequency of 15 Hz. Filtered data was plotted using MATLAB code to produce a stress-strain graph. Stress was calculated by dividing the force measured by the area of the plunger tip, while strain was calculated by a change in the displacement measured by the muscle motor.

A calibration curve was plotted for strain as described above and used to calculate the strain on the tissue based on the displacement measured by the muscle motor.

The elastic modulus, yield strength and failure strength were picked from points on the stress-strain graph generated using MATLAB as described previously.

Statistical analysis

A Student's T-test was conducted to compare the intact retina with the polymer sealed retina in the isolated tissue.

Results

We measured the diameters of the eyes prior to clamping and after clamping to ensure that negligible additional pressure was being generated. The diameters of the eyes for the static testing set were 22.36±0.506 mm unclamped. After clamping, they were 22.23±0.573 mm which was a 0.6% change. While for dynamic testing, the unclamped diameters were 22.55±0.892 mm and the clamped diameters were 22.48±0.798 mm with a 0.3% change.

Static testing of whole porcine eyes

Table 1 summarizes the findings from the static testing of whole eyes. The Young's Modulus (E) for the retina was 278±158 kPa while that for the polymer sealed retina was 2160±923 kPa. The polymer sealed retina was found to be significantly stiffer than intact retina ($p<0.0001$) (Figure 11).

The average Yield strength (Y) was 365 ± 248 kPa for the intact retina and 331 ± 157 kPa for the polymer sealed retina. The yield strength of the polymer sealed retina was not significantly different that of the intact retina ($p = 0.3321$) (Figure 10,11).

The average Failure Strength (F) of the retina was found to be 403 ± 266 kPa while that of the polymer was close at 436 ± 198 kPa. This was not a statistically significant difference ($p = 0.9802$) (Figure 10, 11).

Table 1: Summary of the results from the static tests for intact eyes

STATIC TESTS		
Parameters	Intact Retina (n = 18)	Polymer sealed Retina (n = 21)
Elastic modulus (kPa)	278±158	2160±923
Yield Strength (kPa)	365 ± 248	331 ± 157
Failure Stength (kPa)	403 ± 266	436 ± 198

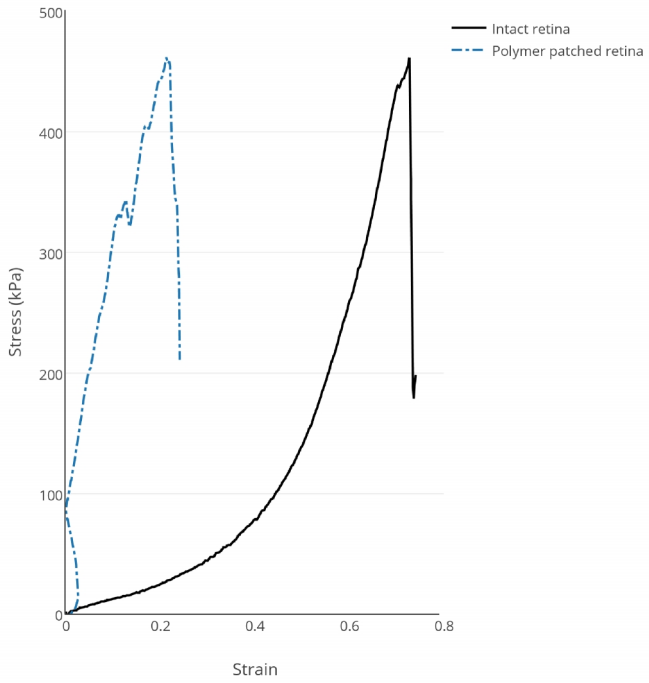

Figure 10. Specimen plot of the stress vs. strain of intact retina and polymer sealed retina static tests conducted on whole porcine eyes by loading up to failure. A steep drop occurs at the point of failure.

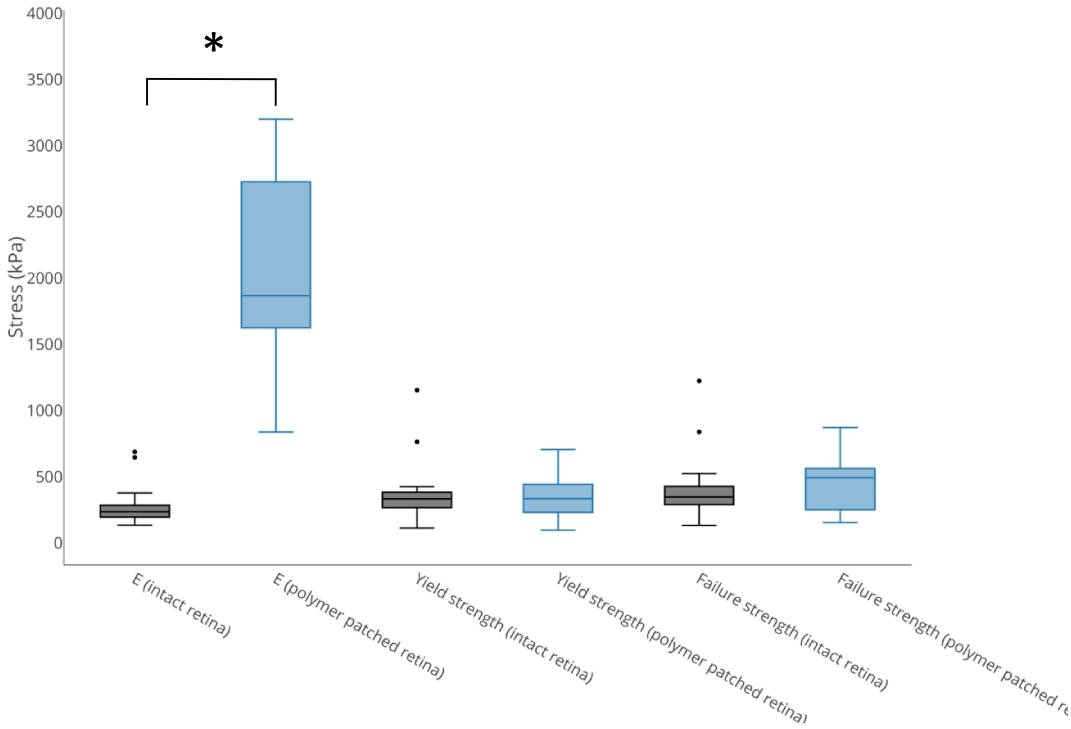

Figure 11. Box plot for elastic modulus, yield strength and failure strength of the intact retina compared to the polymer sealed retina in intact porcine eyes.

(* = statistically significant)

Dynamic testing of whole porcine eyes

As seen in figure 15, the elastic moduli were 116 ± 72.7 kPa for intact retina and 54.5 ± 25.2 kPa for the polymer sealed retina. This difference was statistically significant ($p = 0.0003$). The torn retina had a modulus of 27.2 ± 20 kPa and was significantly less stiff than the intact retina ($p < 0.0001$). However the difference between the elastic moduli of the torn retina compared to that of the polymer sealed retina was not statistically significant ($p = 0.1705$).

Figure 12 shows the load-unload curves for intact, torn and polymer sealed retinas. The hysteresis values were closer between intact retina and polymer sealed retina and were not statistically significant ($p = 0.7132$). Hysteresis for the intact retina was 39.21 ± 4.68 % while that for the polymer sealed retina was 41.89 ± 12.90 %. The hysteresis of the torn retina was significantly lower that the intact retina 49.60 ± 11.96 % ($p < 0.0098$). However the difference between torn and polymer sealed retina was not statistically significant (Figure 14). Resilience was 60.79 ± 4.68 % for the intact retina and 58.11 ± 12.90 % for the polymer sealed retina.

Table 2: Summary of the results from dynamic tests

	DYNAMIC TESTS		
Parameters	Intact Retina (n = 19)	Torn Retina (n = 19)	Polymer sealed Retina (n = 19)
Elastic modulus (kPa)	116 ± 72.7	27.2 ± 20	54.5 ± 25.2
Hysteresis (%)	39.21 ± 4.68	49.60 ± 11.96	41.89 ± 12.90
Resilience (%)	60.79 ± 4.68	50.39 ± 11.97	58.11 ± 12.90

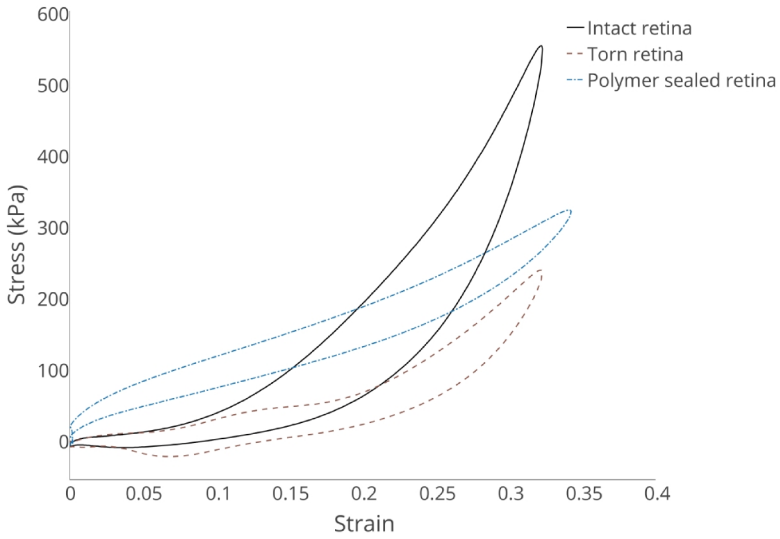

Figure 12. Stress-strain plot of specimen after dynamic testing of the intact retina, torn retina and polymer sealed retina.

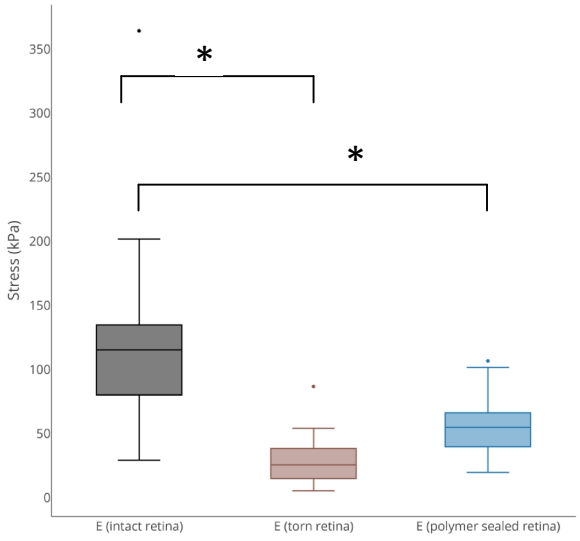

Figure 13. Box plot of the Elastic moduli calculated from dynamic testing * = statistically significant

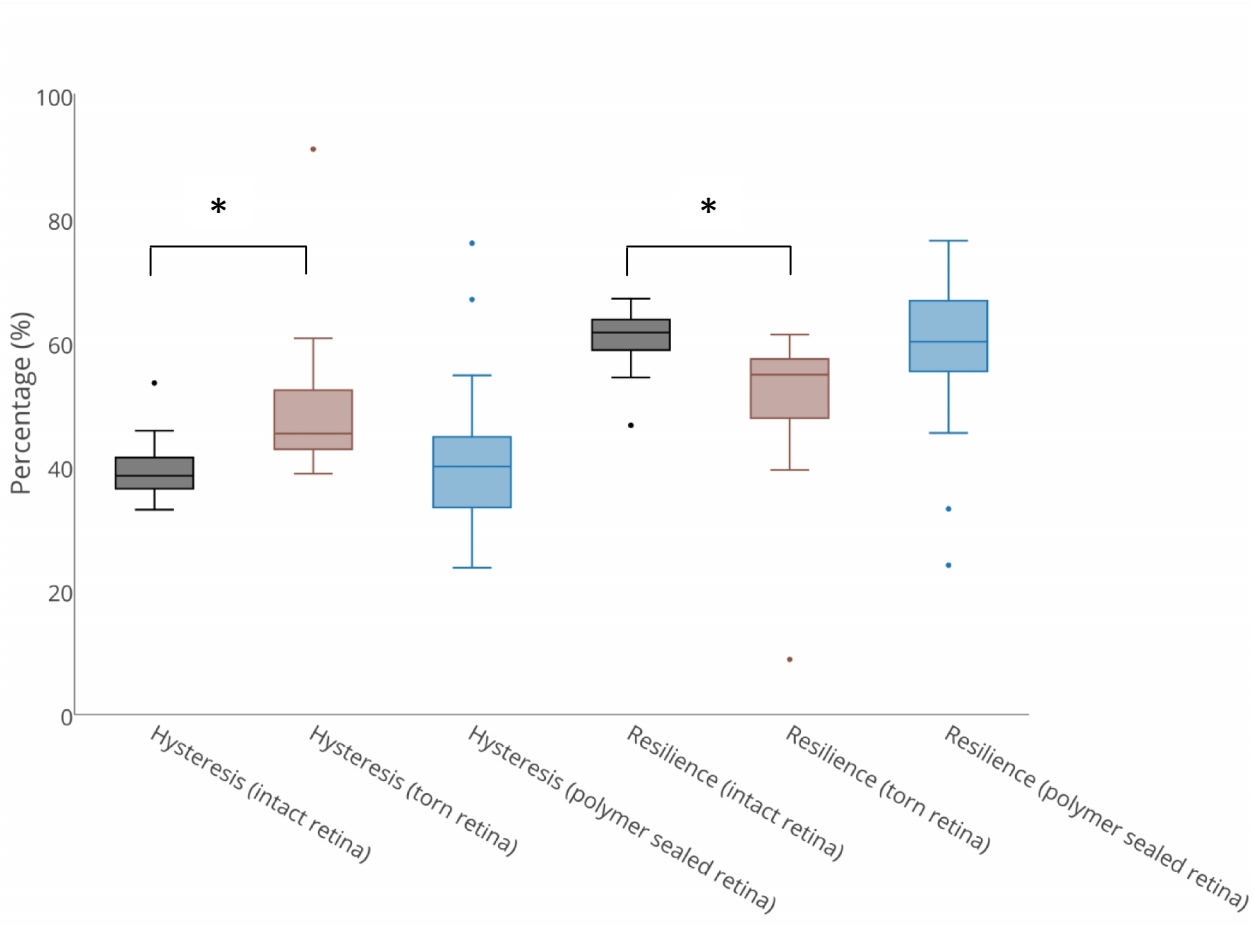

Figure 14. Box plot of hysteresis and resilience from dynamic tests.

(* = statistically significant)

Static testing of the isolated retina

Table 3 presents a summary of the observations from the static testing of the isolated retina. The modulus for the retina was 6.58 ± 5.57 kPa while that for the polymer sealed retina was 36.05 ± 17.26 kPa. The polymer sealed retina was found to be significantly stiffer than intact retina ($p<0.0001$) (Figure 16).

The average Yield strength was 3.77 ± 2.80 kPa for the intact retina and 18.35 ± 7.07 kPa for the polymer sealed retina. The polymer sealed retina's yield strength was found to be significantly different that of the intact retina ($p<0.0001$) (Figure 15, 16).

The average failure strength of the retina was found to be 4.39 ± 3.07 kPa while that of the polymer was a lot higher at 21.44 ± 7.11 kPa. This was a statistically significant difference ($p<0.0001$) (Figure 15,16).

Table 3: Summary of the results from the static tests for isolated retina

	STATIC TESTS	
Parameters	Intact Retina (n = 18)	Polymer sealed Retina (n = 18)
Elastic modulus (kPa)	6.58 ± 5.57	36.05 ± 17.26
Yield Strength (kPa)	3.77 ± 2.80	18.35 ± 7.07
Failure Stength (kPa)	4.39 ± 3.07	21.44 ± 7.11

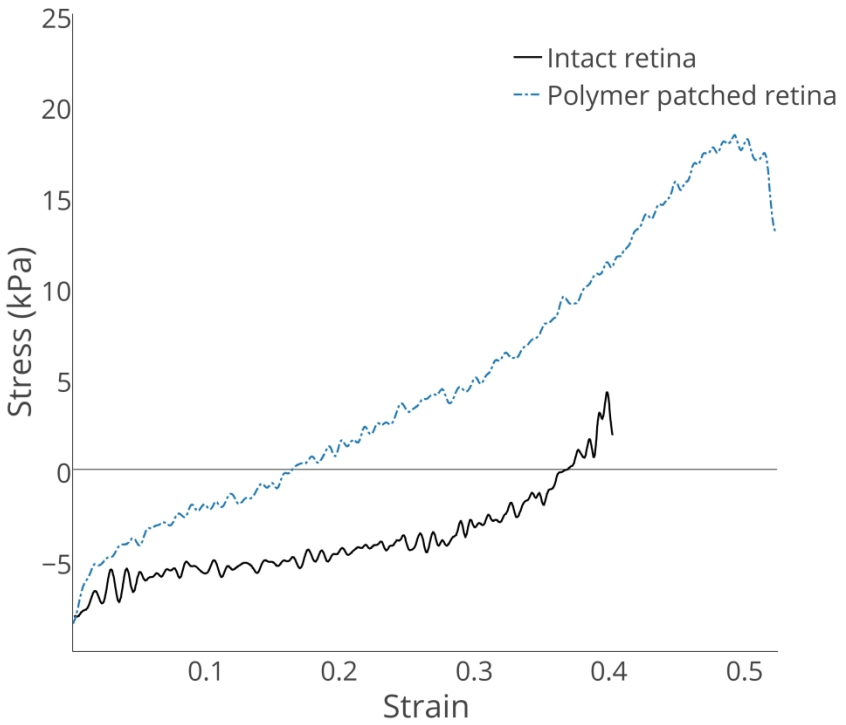

Figure 15. Individual samples from static testing of the isolated retina

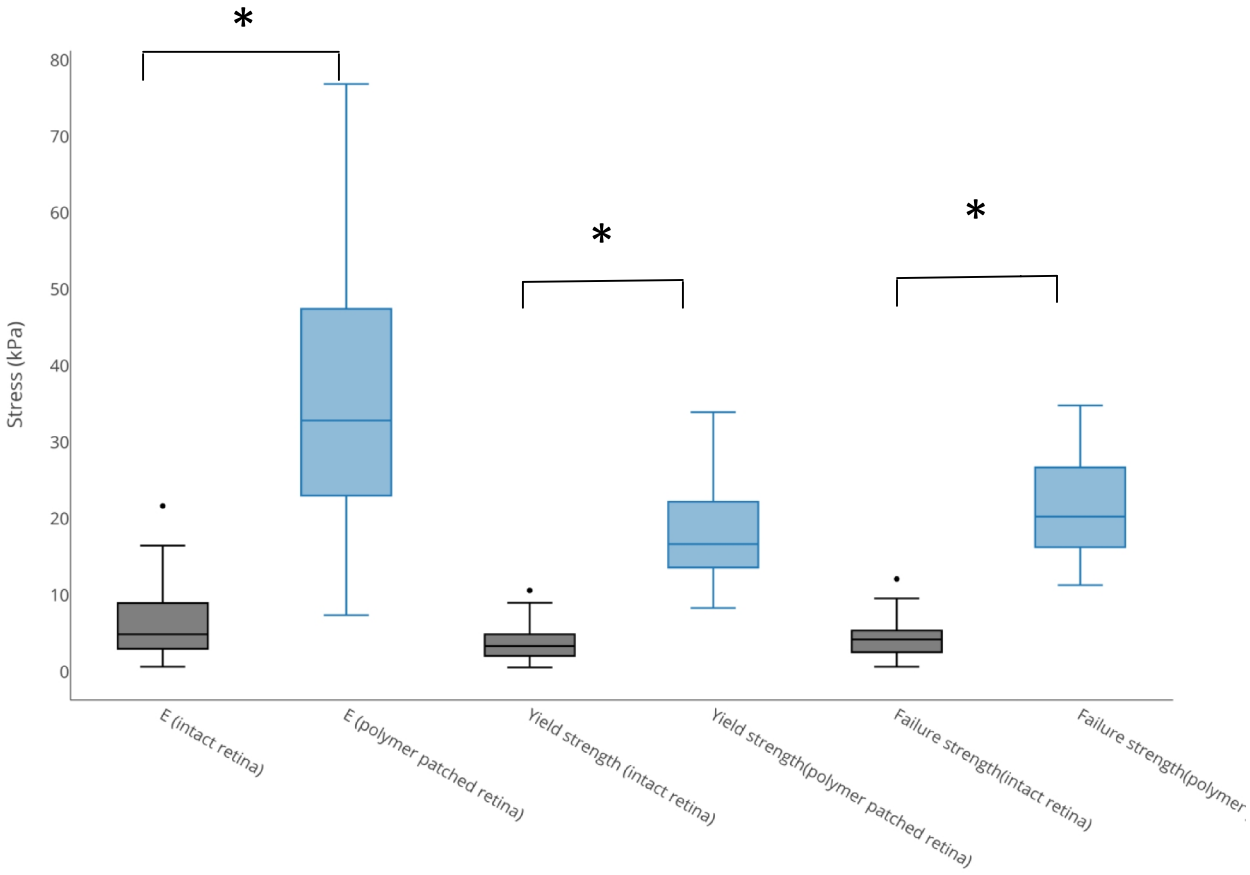

Figure 16. Box plots of Elastic modulus, yield strength and failure strength of the isolated intact retina vs. the isolated polymer sealed retina (* = statistically significant)

Discussion

Static and dynamic testing of intact porcine eyes was carried out to determine how the Medicus polymer performs compared to normal retinal tissue. In these experiments we treated the retina in a nearly intact eye as the standard to be met by the polymer. This is the first time that experiments of this kind were carried out on an intact eye without removal or isolation of tissues. We also carried out isolated retina experiments to understand the impact of the whole eye preparation compared to isolated tissue and to compare our results with prior studies done on the isolated retina.

Overall, the Medicus Polymer exhibits a significant difference in the elastic modulus compared to the intact retina in both the whole eye preparation and the isolated retina preparation. However, contradictory results were revealed when comparing the static and dynamic testing. Despite this difference in elastic moduli, the Medicus polymer was successful in mimicking the yield strength, failure strength, and resilience of the intact tissues when tested under static and dynamic conditions in both whole eye and isolated retinal preparations.

The static tests show that the polymer is significantly stiffer than the intact tissues and this could be an important factor when the polymer is used as an adhesive for the detached retina. Having a stiffer polymer will mean additional strains on the neighbouring tissues that could lead to further re-deatchments [67, 85].

The values calculated in the static testing of retina in whole eyes are very similar to those reported previously from isolated retina experiments in the literature [75], [76], [78]. These previous studies had tested the retina in tension along an axis that lay

within the plane of the tissue which has been shown to be highly variable depending on the direction of the dissection and applied force [76]. In our whole eye experiments, the axis of testing was perpendicular to the retina which is more biologically relevant if we consider trauma to the eyeball or traction from a collapsing vitreous. One of the major variables remains how dissection was done. For our experiments, while the choroid was removed, the RPE and its basement membrane was in place, and this probably explains the differences between the elastic modulus of retina obtained by intact eye testing (278 ± 158 kPa) which is several times greater than the values of isolated retina testing (6.58 ± 5.57 kPa). It is possible that the dissection in the previous studies did not entirely eliminate the basement membrane and RPE. The values for the isolated retina are very close to the 10kPa reported by Worthington *et al.* while those from the whole eye experiments are also within the range of 100-300 kPa reported by previous studies done on porcine retina at 25º C in saline [23, 75, 76, 78].

As seen in Figure 12, we also saw that the stress-strain curves for the isolated retina begin below 0 mN. This is probably due to the fact that when the retina was attached to the rim of the cylinder, it was not always taut. While we positioned the plunger as close to the retina as possible, the lever arm did not register any force until the plunger had pushed down a little further and registered some resistance. Also, there is the possibility of microfractures in the tissue during dissection from the rest of the eye.

The results from whole eye preparation dynamic testing contradict those from whole eye static testing revealing a significantly lower elastic modulus of the polymer compared to the retina (Figure 13). This could be explained in part by the shredding behavior of the polymer. It was observed that as the plunger cyclically loaded the

polymer, areas around the edge of the plunger began tear. These tears possibly reduce the strength of the polymer and therefore its stiffness. It is also possible the difference in modulus is due to some damping, or stress-thinning, properties of the polymer that have not yet been identified. Further experiments to understand the storage and loss moduli of the Medicus polymer would be a useful next step [86].

The values from static testing for the intact retina from whole eyes and the isolated retina are consistent and fall in the 100-300 kPa range, however the elastic moduli of the polymer sealed retina seem to contradict each other. Considering the fact that the polymer underwent tearing during every successive cycle of dynamic testing, the values recorded by static testing seem to be more relevant. Dynamic testing gave us relevant values for the elastic modulus and hysteresis values of the intact retina.

We also found consistency in the comparative difference in the stiffness of the polymer and in intact retina in both, whole eyes and isolated retina, where the polymer showed up as significantly stiffer than the retina. The dynamic testing of the polymer should be redone to test and see whether differences in the frequency of testing or number of cycles will yield relevant results with minimal destruction of the polymer.

About the experimental setup

We see large errors for the results obtained by static and dynamic testing. One of the reasons this occurs is due to individual variation in each eye. In a previous work, it was seen that the retina is an anisotropic, inhomogenous tissue with a difference in the elastic moduli of adjacent areas attributed to the distribution of compliant nerve fiber bundles and stiff neuronal cell bodies in the inner retina [87]. In addition, the retinal vasculature has been shown to change the local mechanical properties of the

retina. The retina was found to be stiffer where blood vessels were present and the variation was greater if the blood vessels were larger in size [77]. Neither of these factors were controlled for in the present study.

The thickness of polymer that was applied and cured on the scleral window also varied between 1 – 2 mm and there was no way of measuring the thickness without upsetting the hydrogel. We also believe that the difference in the elastic moduli of the polymer obtained from static and dynamic testing is due to the experimental design and further modification of the experimental parameters will yield more relevant results from dynamic testing.

Conclusion

The Medicus Polymer is a tissue adhesive hydrogel developed by Medicus Biosciences that adheres well to tissues and is optically clear. Being a hydrogel, it can be tuned to match its biomechanical properties to the tissue it is helping heal. We developed a novel experimental design to test the retina *in situ* in an intact porcine eye and compare the biomechanical parameters to those of a torn sealed retina with the polymer.

The current formulation of the polymer does not match the intact retina in its elastic modulus although it has similar failure and yield strengths as well as resilience. If the polymer can be tuned to better mimic the intact retina, this polymer may help treat existing tears and detachments, and prevent further re-detachments due to a mismatch in biomechanical parameters.

Bibliography

[1] K. Chen, A. P. Rowley, J. D. Weiland, and M. S. Humayun, "Elastic properties of human posterior eye.," *Journal of Biomedical Materials Research Part A*, vol. 102, no. 6, pp. 1–7, Jul. 2013.

[2] M. H. Haimann, T. C. Burton, and C. K. Brown, "Epidemiology of retinal detachment.," *Archives of Ophthalmology*, vol. 100, no. 2, pp. 289–92, Feb. 1982.

[3] R. Dyson and A. Fitt, "Post re-attachment retinal re-detachment," In: *Proceedings of the Fourth Medical Study Group, University of Strathclyde, Glasgow,* 14th-17th September, 2004.

[4] L. Remington, *Clinical anatomy of the visual system*. Elsevier Health Sciences 2011.

[5] N. M. Holekamp, "The vitreous gel: more than meets the eye.," *American Journal of Ophthalmology*, vol. 149, no. 1, pp. 32–6, Jan. 2010.

[6] N. R. Galloway, W. M. K. Amoaku, P. H. Galloway, and A. C. Browning, *Common Eye Diseases and their Management*. 2006, pp. 7–15.

[7] M. M. Le Goff and P. N. Bishop, "Adult vitreous structure and postnatal changes.," *Eye (Lond).*, vol. 22, no. 10, pp. 1214–22, Oct. 2008.

[8] T. L. Ponsioen, J. M. M. Hooymans, and L. I. Los, "Remodelling of the human vitreous and vitreoretinal interface--a dynamic process.," *Progress in Retinal and Eye Research*, vol. 29, no. 6, pp. 580–95, Nov. 2010.

[9] G. Eisner, "The anatomy and biomicroscopy of the vitreous body," *New Developments in Ophthalmology Nijmegen*, pp. 16–18, Oct. 1975.

[10] M. Kita and M. F. Marmor, "Retinal adhesive force in living rabbit, cat, and monkey eyes. Normative data and enhancement by mannitol and acetazolamide.," *Investigative Ophthalmology & Visual Science*, vol. 33, no. 6, pp. 1879–82, May 1992.

[11] M. F. Marmor and T. Maack, "Local environmental factors and retinal adhesion in the rabbit.," *Experimental Eye Research*, vol. 34, no. 5, pp. 727–33, May 1982.

[12] M. Marmor, "Retinal detachment from hyperosmotic intravitreal injection," *Investigative Ophthalmology & Visual Science*, vol. 18, no. 12, pp. 1237–1244, 1979.

[13] M. R. Allansmith, C. R. Whitney, B. H. Mcclellan, and L. P. Newman, "Immunoglobulins in the Human Eye," *Archives of Ophthalmology,* vol. 89, no.1, pp. 36-45, Jan. 1973.

[14] K. Emi, J. E. Pederson, and C. B. Toris, “Hydrostatic pressure of the suprachoroidal space.,” *Investigative Ophthalmology & Visual Science*, vol. 30, no. 2, pp. 233–8, Feb. 1989.

[15] C. D. Toris, J. E. Pederson, S. Tsuboi, D. S. Gregerson, and T. J. Rice, “Extravascular Albumin Concentration of the Uvea,” *Investigative Ophthalmology & Visual Science* , vol. 31, no. 1, pp. 43–53, Jan. 1990.

[16] A. Alm and S. F. E. Nilsson, “Uveoscleral outflow--a review.,” *Experimental Eye Research*, vol. 88, no. 4, pp. 760–8, Apr. 2009.

[17] I. Fatt and K. Shantinath, “Flow conductivity of retina and its role in retinal adhesion.,” *Experimental Eye Research*, vol. 12, no. 2, pp. 218–26, Sep. 1971.

[18] B. Kirchhof and S. J. Ryan, “Differential permeance of retina and retinal pigment epithelium to water: implications for retinal adhesion.,” *International Ophthalmology,* vol. 17, no. 1, pp. 19–22, Feb. 1993.

[19] H. M. S. and Kinsey, Everrett (Howe Laboratory of Ophthalmology, M. E. and E. Infirmary), M. Grant, and D. Cogan, “Water movement and the eye,” *Archives of Ophthalmology*, vol. 27, no. 2, pp. 242–252, 1942.

[20] W. S. Foulds, “Is your vitreous really necessary? The role of the vitreous in the eye with particular reference to retinal attachment, detachment and the mode of action of vitreous substitutes.,” *Eye (Lond).*, vol. 1 (Pt 6), no. December 1985, pp. 641–64, Jan. 1987.

[21] R. Foos, “Vitreoretinal juncture; epiretinal membranes and vitreous.,” *Investigative Ophthalmology & Visual Science*, vol. 16, no. 5, pp. 416–422, 1977.

[22] R. Foos, “Vitreoretinal juncture; topographical variations,” *Investigative Ophthalmology & Visual Science*, vol. 11, no. 10, pp. 801–808, 1972.

[23] G. Wollensak, E. Spoerl, G. Grosse, and C. Wirbelauer, “Biomechanical significance of the human internal limiting lamina,” *Retina*, vol. 26, no.8, pp. 965-968 Oct 2006.

[24] B. Rosengren and S. Österlin, “Hydrodynamic events in the vitreous,” *Ophthalmologica Basel*, no. 173, pp. 513–524, 1976.

[25] F. Mutlu and I. H. Leopold, “The structure of human retinal vascular system.,” *Archives of Ophthalmology*, vol. 71, pp. 93–101, Jan. 1964.

[26] D.-Y. Yu, S. J. Cringle, and E.-N. Su, “Intraretinal oxygen distribution in the monkey retina and the response to systemic hyperoxia.,” *Investigative Ophthalmology & Visual Science*, vol. 46, no. 12, pp. 4728–33, Dec. 2005.

[27] X. Y. Yao, E. G. Endo, and M. F. Marmor, “Reversibility of retinal adhesion in the rabbit.,” *Investigative Ophthalmology & Visual Science*, vol. 30, no. 2, pp. 220–4, Feb. 1989.

[28] G. Hageman, M. Marmor, and X. Y. Yao, “The interphotoreceptor matrix mediates primate retinal adhesion,” *Archives of Ophthalmology*, no. 113, pp. 655–660, 1995.

[29] L. V Johnson, G. Hogemon, and J. C. Blonks, “Interphotoreceptor Matrix Domains Ensheath Vertebrate Cone Photoreceptor Cells,” *Investigative Ophthalmology & Visual Science* vol. 27, no. 2, pp. 129-135, Feb. 1986.

[30] H. Zauberman and H. DeGuillebon, “Retinal traction in vivo and postmortem.,” *Archives of Ophthalmology*, vol. 87, no. 5, pp. 549–54, May 1972.

[31] M. F. Marmor, “Mechanisms of retinal adhesion,” *Progress in Retinal Research*, vol. 12, pp. 179–204, Jan. 1993.

[32] T. Wolfensberger, “The retinal pigment epithelium: Current aspects of function and disease,” M. Marmor, Ed. New York: Oxford University Press, 1998, pp. 420–438.

[33] A. Negi and M. F. Marmor, “Quantitative estimation of metabolic transport of subretinal fluid.,” *Investigative Ophthalmology & Visual Science*, vol. 27, no. 11, pp. 1564–8, Nov. 1986.

[34] M. Marmor and X. Yao, “The metabolic dependency of retinal adhesion in rabbit and primate,” *Archives of Ophthalmology*, no. 113, pp. 232–238, 1995.

[35] M. F. Marmor, A. S. Abdul-rahim, and D. S. Cohen, “The effect of metabolic inhibitors on retinal adhesion and subretinal fluid resorption,” *Investigative Ophthalmology & Visual Science,* vol. 19, no. 8, pp. 893–903, Aug. 1980.

[36] D. Brinton and C. Wilkinson, “Retinal Detachment: Priniciples and Practice,” 3rd edition, 2009.

[37] N. E. Byer, “What happens to untreated asymptomatic retinal breaks, and are they affected by posterior vitreous detachment?,” *Ophthalmology*, vol. 105, no. 6, pp. 1045–9; discussion 1049–50, Jun. 1998.

[38] J. Sebag, “Age-related differences in the human vitreoretinal interface.,” *Archives of Ophthalmology*, vol. 109, no. 7, pp. 966–71, Jul. 1991.

[39] R. I. Angunawela, A. Azarbadegan, G. W. Aylward, and I. Eames, “Intraocular fluid dynamics and retinal shear stress after vitrectomy and gas tamponade.,” *Investigative Ophthalmology & Visual Science*, vol. 52, no. 10, pp. 7046–51, Sep. 2011.

[40] J. Sebag, “Anatomy and pathology of the vitreo-retinal interface.,” *Eye (Lond).*, vol. 6 (Pt 6), pp. 541–52, Jan. 1992.

[41] a Takeuchi, G. Kricorian, and M. F. Marmor, “Albumin movement out of the subretinal space after experimental retinal detachment.,” *Investigative Ophthalmology & Visual Science*, vol. 36, no. 7, pp. 1298–305, Jun. 1995.

[42] A. Takeuchi, G. Kricorian, and M. Marmor, “When vitreous enters the subretinal space,” *Retina*, no. 16, pp. 426–430, 1996.

[43] A. Takeuchi, G. Kricorian, X. Y. Yao, J. W. Kenny, and M. F. Marmor, “The rate and source of albumin entry into saline-filled experimental retinal detachments.,” *Investigative Ophthalmology & Visual Science*, vol. 35, no. 11, pp. 3792–8, Oct. 1994.

[44] N. E. Byer, “Clinical study of retinal breaks.,” *Transactions: American Academy of Ophthalmology & Otolaryngology*, vol. 71, no. 3, pp. 461–73, Jan. 1967.

[45] N. Byer, “The natural history of asymptomatic retinal breaks,” *Ophthalmology*, vol. 89, no. 9, pp. 1033–1039, 1982.

[46] M. F. Marmor, “New hypotheses on the pathogenesis and treatment of serous retinal detachment,” *Graefe's Archive for Clinical and Experimental Ophthalmology,* vol. 226, no. 6, pp. 548–552, 1988.

[47] M. F. Marmor, “Control of subretinal fluid: experimental and clinical studies.,” *Eye (Lond).*, vol. 4 (Pt 2), pp. 340–4, Jan. 1990.

[48] A. Negi and M. F. Marmor, “The resorption of subretinal fluid after diffuse damage to the retinal pigment epithelium.,” *Investigative Ophthalmology & Visual Science*, vol. 24, no. 11, pp. 1475–9, Nov. 1983.

[49] X. Lin, J. Ge, Q. Gao, Z. Wang, C. Long, L. He, Y. Liu, and Z. Jiang, “Evaluation of the flexibility, efficacy, and safety of a foldable capsular vitreous body in the treatment of severe retinal detachment.,” *Investigative Ophthalmology & Visual Science*, vol. 52, no. 1, pp. 374–81, Jan. 2011.

[50] A. Nishimura, M. Kimura, Y. Saito, and K. Sugiyama, “Efficacy of primary silicone oil tamponade for the treatment of retinal detachment caused by macular hole in high myopia.,” *American Journal of Ophthalmology*, vol. 151, no. 1, pp. 148–55, Jan. 2011.

[51] D. J. D’Amico, “Primary Retinal Detachment,” *New England Journal of Medicine*, no. 359, pp. 2346–2354, Nov. 2008.

[52] A. Negi and M. F. Marmor, “Healing of photocoagulation lesions affects the rate of subretinal fluid resorption.,” *Ophthalmology*, vol. 91, no. 12, pp. 1678–83, Dec. 1984.

[53] F. Bandello and M. B. Parodi, *Surgical Retina*, vol. 2. Karger Medical and Scientific Publishers, 2012.

[54] M. Kita, A. Negi, S. Kawano, and Y. Honda, "Photothermal, cryogenic, and diathermic effects of retinal adhesive force in vivo.," *Retina*, vol. 11, no. 4, pp. 441–444, 1991.

[55] N. M. Holekamp, Y.-B. Shui, and D. C. Beebe, "Vitrectomy surgery increases oxygen exposure to the lens: a possible mechanism for nuclear cataract formation.," *American Journal of Ophthalmology*, vol. 139, no. 2, pp. 302–10, Feb. 2005.

[56] A. Teixeira, L. P. Chong, N. Matsuoka, L. Arana, R. Kerns, P. Bhadri, and M. Humayun, "Vitreoretinal traction created by conventional cutters during vitrectomy.," *Ophthalmology*, vol. 117, no. 7, pp. 1387–92.e2, Jul. 2010.

[57] H. H. Ghoraba and A. I. Zayed, "Suprachoroidal hemorrhage as a complication of vitrectomy.," *Ophthalmic Surgery and Lasers*, vol. 32, no. 4, pp. 281–8, Jan. 2001.

[58] J. Ambati and J. Arroyo, "Postoperative complications of scleral buckling surgery," *International Ophthalmology Clinics*, vol. 40, no. 1, pp. 175–185, 2000.

[59] Y.-J. Peng, Y.-T. Lu, K.-S. Liu, S.-J. Liu, L. Fan, and W.-C. Huang, "Biodegradable balloon-expandable self-locking polycaprolactone stents as buckling explants for the treatment of retinal detachment: an in vitro and in vivo study.," *Journal of Biomedical Materials Research Part A*, vol. 101, no. 1, pp. 167–75, Jan. 2013.

[60] W. Hawkins and C. Schepens, "Choroidal detachment and retinal surgery: a clinical and experimental study," *American Journal of Ophthalmology*, no. 62, pp. 813–819, 1966.

[61] M. Roldán-Pallarés, J. L. del Castillo Sanz, S. Awad-El Susi, and M. F. Refojo, "Long-term complications of silicone and hydrogel explants in retinal reattachment surgery.," *Archives of Ophthalmology*, vol. 117, no. 2, pp. 197–201, Feb. 1999.

[62] I. D. Fabian and J. Moisseiev, "Complications of pneumatic retinopexy--reply.," *JAMA ophthalmology*, vol. 131, no. 10. pp. 1370–1, Oct-2013.

[63] J. Haut, M. Ullern, M. Chermet, and G. Van Effenterre, "Complications of intraocular injections of silicone combined with vitrectomy," *Ophthalmologica*, no. 180, pp. 29–35, 1980.

[64] S. F. Al-Wadani, M. a Abouammoh, and A. M. Abu El-Asrar, "Visual and anatomical outcomes after silicone oil removal in patients with complex retinal detachment.," *International Ophthalmology*, no. 180, pp. 29–35, 1980.

[65] N. Bülow, “The process of wound healing of the avascular outer layers of the retina. Light- and electron microscopic studies on laser lesions of monkey eyes.,” *Acta Ophthalmologica Suppl. (Oxf.).*, no. 139, pp. 7–60, 1978.

[66] M. Mehdizadeh and J. Yang, “Design strategies and applications of tissue bioadhesives.,” *Macromolecular Bioscience*, vol. 13, no. 3, pp. 271–88, Mar. 2013.

[67] T. Hida, S. M. Sheta, A. D. Proia, and B. W. McCuen, “Retinal toxicity of cyanoacrylate tissue adhesive in the rabbit.,” *Retina*, vol. 8, no. 2, pp. 148–153, 1988.

[68] M. J. Colthurst, R. L. Williams, P. S. Hiscott, and I. Grierson, “Biomaterials used in the posterior segment of the eye.,” *Biomaterials*, vol. 21, no. 7, pp. 649–65, Apr. 2000.

[69] F. Baino, “Towards an ideal biomaterial for vitreous replacement: Historical overview and future trends.,” *Acta Biomaterialia*, vol. 7, no. 3, pp. 921–35, Mar. 2011.

[70] K. E. Swindle, P. D. Hamilton, and N. Ravi, “In situ formation of hydrogels as vitreous substitutes: Viscoelastic comparison to porcine vitreous.,” *Journal of Biomedical Materials Research Part A*, vol. 87, no. 3, pp. 656–65, Dec. 2008.

[71] S. H. Askari and Y. S. CHOI, “Biocompatible hydrogel treatments for retinal detachment,” *US Pat App PCT/US2013/040619*, 2013.

[72] Zalipsky Samuel and Harris J. Milton, *Poly(ethylene glycol)*, vol. 680. Washington, DC: American Chemical Society, 1997, pp. 1–13.

[73] Working Peter K., Newman Mary S., Johnson Judy, and Cornacoff Joel B., *Poly(ethylene glycol)*, vol. 680. Washington, DC: American Chemical Society, 1997, pp. 45–57.

[74] S. Askari and G. Horng, “In-vivo gelling pharmaceutical pre-formulation,” *US Pat. App. 13/696,032*, vol. 1, no. 61, 2011.

[75] K. Chen and J. D. Weiland, “Mechanical characteristics of the porcine retina in low temperatures.,” *Retina*, vol. 32, no. 4, pp. 844–7, Apr. 2012.

[76] K. Chen, A. P. Rowley, and J. D. Weiland, “Elastic properties of porcine ocular posterior soft tissues.,” *Journal of Biomedical Materials Research Part A*, vol. 93, no. 2, pp. 634–45, May 2010.

[77] K. Chen and J. D. Weiland, “Anisotropic and inhomogeneous mechanical characteristics of the retina.,” *Journal of Biomechanics*, vol. 43, no. 7, pp. 1417–21, May 2010.

[78] G. Wollensak and E. Spoerl, “Biomechanical characteristics of retina,” *Retina*, vol. 24, no. 6, pp. 967-970, Dec. 2004.

[79] K. S. Worthington, L. A. Wiley, A. M. Bartlett, E. M. Stone, R. F. Mullins, A. K. Salem, C. A. Guymon, and B. A. Tucker, “Mechanical properties of murine and porcine ocular tissues in compression.,” *Experimental Eye Research*, vol. 121, pp. 194–9, Apr. 2014.

[80] R. Friberg and W. Lace, “A comparison of the elastic properties of human choroid and sclera,” *Experimental Eye Research*, vol. 47, no. 3, pp. 429–436, Sep. 1988.

[81] C. S. Nickerson, J. Park, J. a Kornfield, and H. Karageozian, “Rheological properties of the vitreous and the role of hyaluronic acid.,” *Journal of Biomechanics*, vol. 41, no. 9, pp. 1840–6, Jan. 2008.

[82] P. Sharif-Kashani, J.-P. Hubschman, D. Sassoon, and H. P. Kavehpour, “Rheology of the vitreous gel: effects of macromolecule organization on the viscoelastic properties.,” *Journal of Biomechanics*, vol. 44, no. 3, pp. 419–23, Feb. 2011.

[83] P. Fratzl, *Collagen: structure and mechanics*. Vol. 1. New York:: Springer 2008.

[84] M. R. ROACH and A. C. BURTON, “The reason for the shape of the distensibility curves of arteries.,” *Canadian Journal of Biochemistry & Physiology*, vol. 35, no. 8, pp. 681–690, 1957.

[85] L. Wickham, G. O. Ho-Yen, C. Bunce, D. Wong, and D. G. Charteris, “Surgical failure following primary retinal detachment surgery by vitrectomy: risk factors and functional outcomes.,” *British Journal of Ophthalmology*, vol. 95, no. 9, pp. 1234–8, Sep. 2011.

[86] J. J. Roberts, A. Earnshaw, V. L. Ferguson, and S. J. Bryant, “Comparative study of the viscoelastic mechanical behavior of agarose and poly(ethylene glycol) hydrogels.,” *Journal of Biomedical Materials Research Part B: Applied Biomaterials*, vol. 99, no. 1, pp. 158–69, Oct. 2011.

[87] K. Franze, M. Francke, K. Günter, A. F. Christ, N. Körber, A. Reichenbach, and J. Guck, “Spatial mapping of the mechanical properties of the living retina using scanning force microscopy,” *Soft Matter*, vol. 7, no. 7, p. 3147, 2011.